

Supplementary Materials

CuS Co-catalyst Modified Hydrogenated SrTiO₃ Nanoparticles as an Efficient Photocatalyst for H₂ Evolution

Diwen Zhou^{a,b#}, Ganyu Wang^{a,b#}, Yuan Feng^{a,b}, Wenqian Chen^{a,b*}, Jinyi Chen^{a,b},
Zhichong Yu^{a,b}, Yu Zhang^{a,b}, Jiajun Wang^{a,b}, Liang Tang^{a,b*}

^a Key Laboratory of Organic Compound Pollution Control Engineering, Ministry of
Education, Shanghai 200444, PR China

^b School of Environmental and Chemical Engineering, Shanghai University, Shanghai
200444, PR China

* Corresponding author. E-mail addresses: wenqianchen@shu.edu.cn (W. Chen)
tang1liang@shu.edu.cn (L. Tang)

Equal contribution

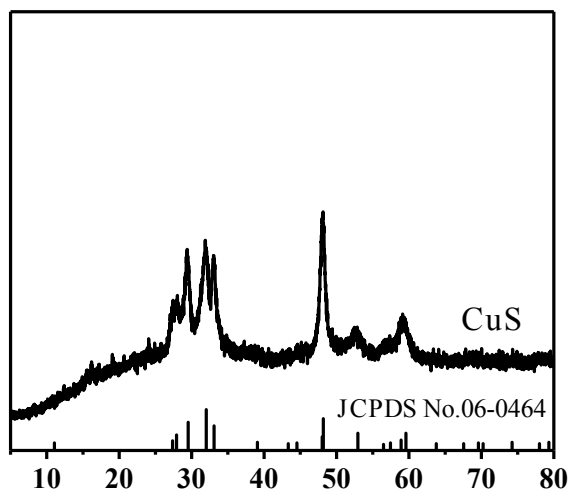


Fig. S1. XRD patterns of pure CuS.

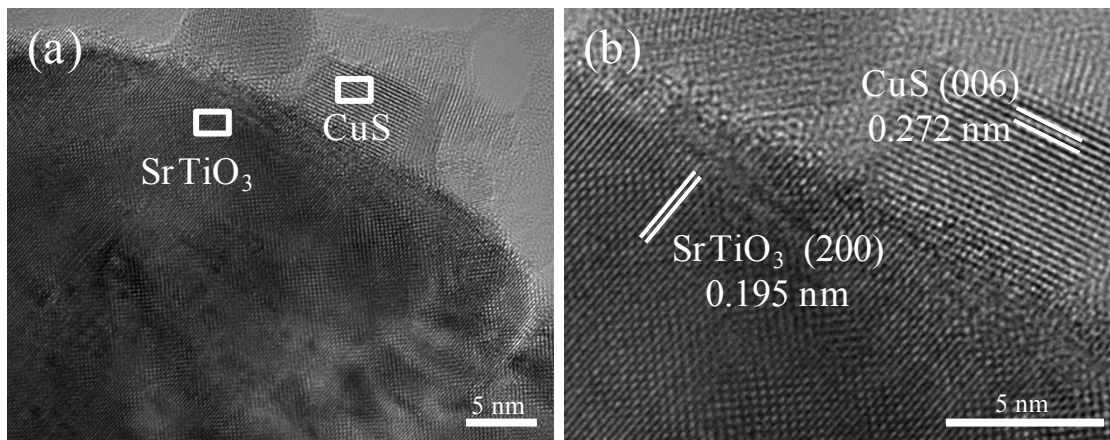


Fig. S2. TEM images of the CuS/STO-350 nanocomposite.

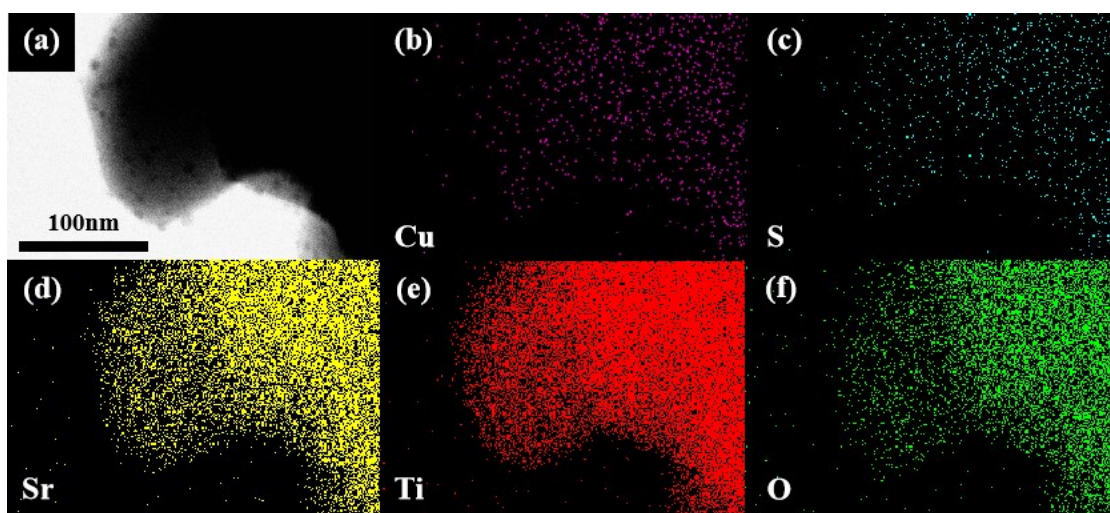


Fig. S3. (a) TEM images of the CuS/STO-350 nanocomposite; Elemental mappings of (b) Cu, (c) S, (d) Sr, (e) Ti and (f) O in CuS/STO-350 nanocomposite.

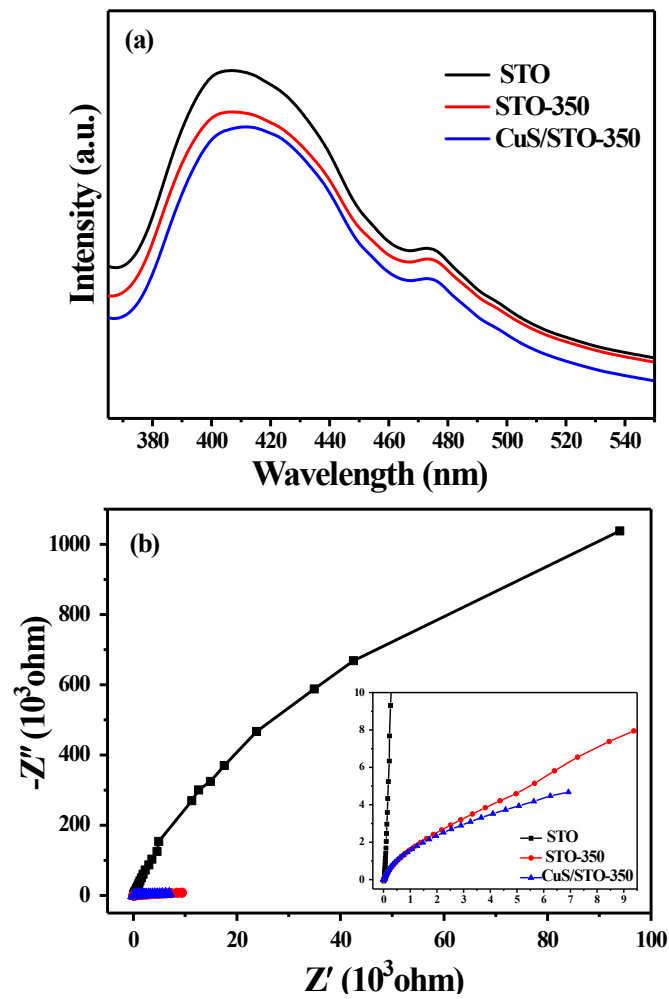


Fig. S4. (a) Photoluminescence spectra (PL); (b) Electrochemical impedance spectroscopy(EIS) of SrTiO_3 , STO-350, and CuS/STO-350 nanocomposites.

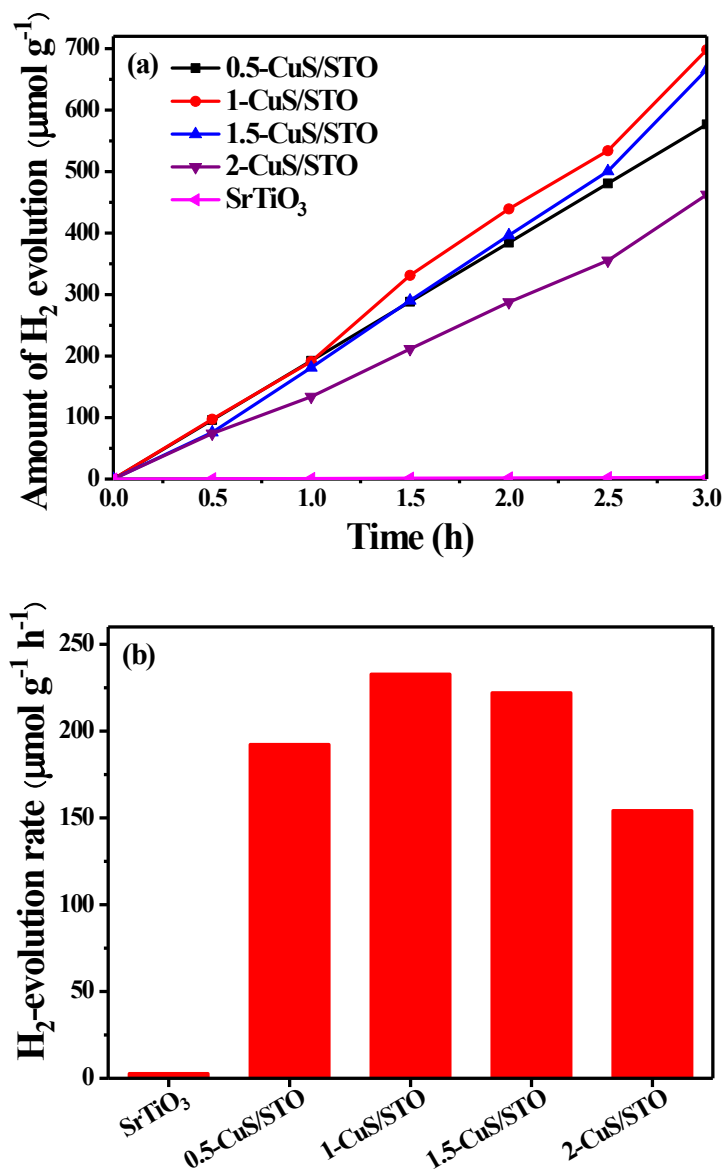


Fig. S5. (a) Time-dependent amounts of photocatalytic H_2 evolution and (b) H_2 evolution rates over SrTiO_3 and CuS/STO nanocomposites.

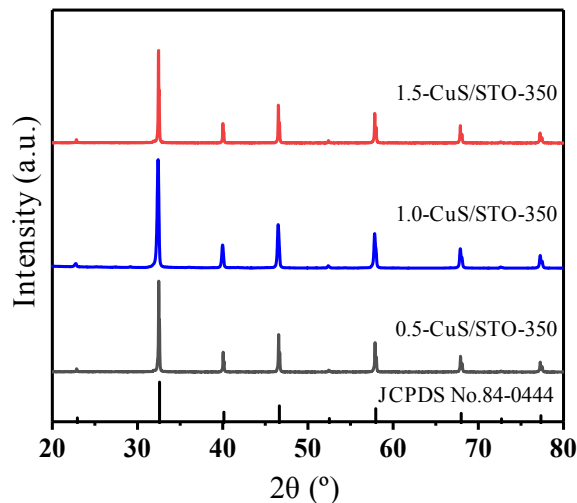


Fig. S6. XRD patterns of 0.5-CuS/STO-350, 1.0-CuS/STO-350 (CuS/STO-350) and 1.5-CuS/STO-350.

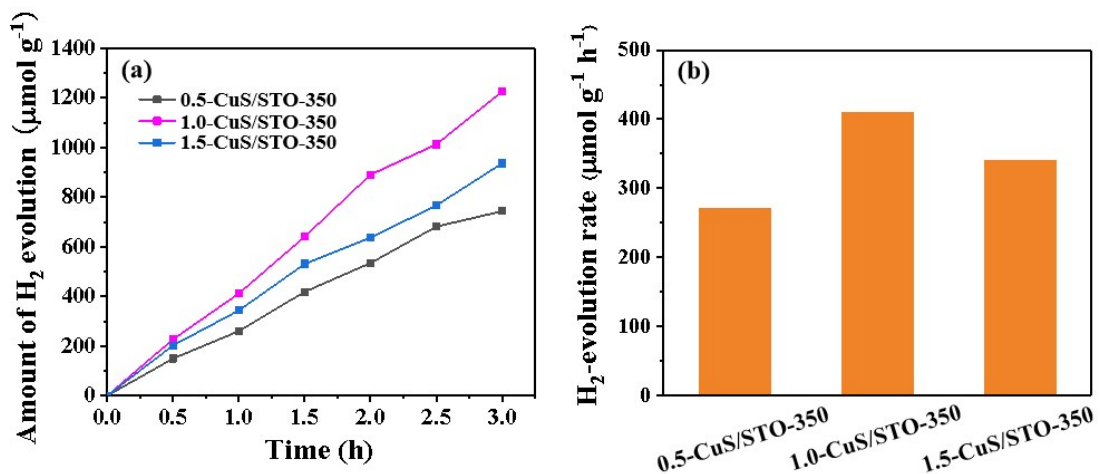


Fig. S7. (a) Time-dependent amounts of photocatalytic H₂ evolution over different photocatalysts; (b) H₂ evolution rates of different photocatalysts.

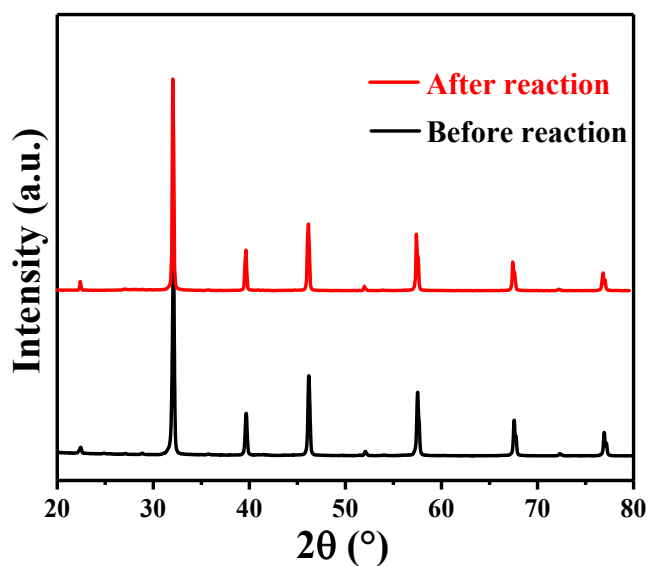


Fig. S8. XRD patterns of CuS/STO-350 nanocomposite before and after the photocatalytic reaction.

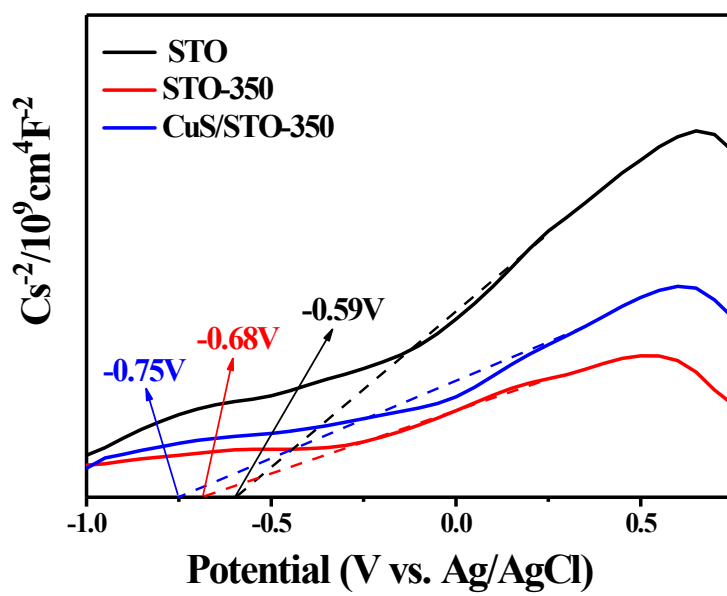


Fig. S9. Mott–Schottky plots of SrTiO_3 , STO-350 and CuS/STO-350 nanocomposites.

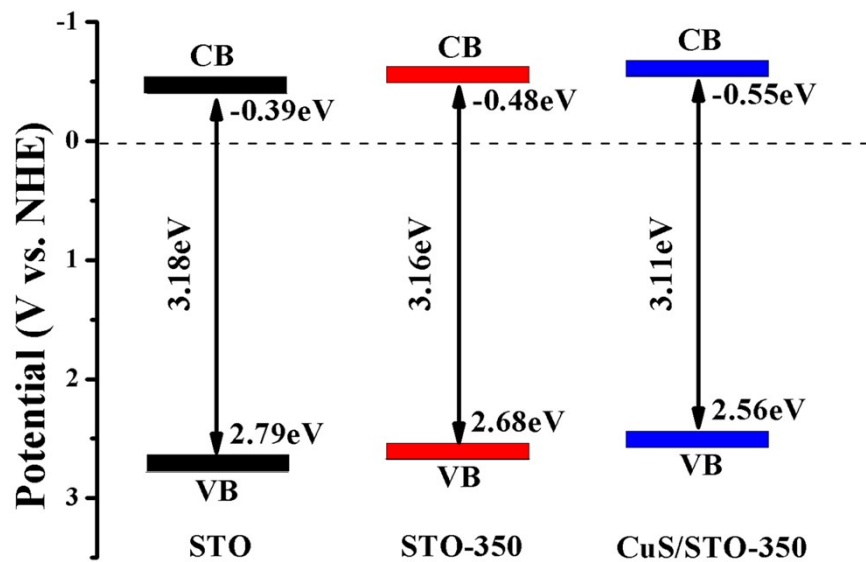


Fig. S10. Estimated band-gap diagram of pure SrTiO₃, STO-350 and CuS/STO-350 nanocomposites.